Carcinogenesis vol.26 no.6 pp.1055–1063, 2005
doi:10.1093/carcin/bgi060
Advance Access publication March 17, 2005

Estrogen or antiprogestin treatment induces complete regression of pulmonary and axillary metastases in an experimental model of breast cancer progression

Silvia I.Vanzulli[2,†], Rocío Soldati[1,†], Roberto Meiss[2], Lucas Colombo[3], Alfredo A.Molinolo[1,4] and Claudia Lanari[1,*]

[1]Laboratory of Hormonal Carcinogenesis, Instituto de Biología y Medicina Experimental, CONICET (Consejo Nacional de Investigaciones Científicas y Técnicas), Buenos Aires, Argentina, [2]Instituto de Estudios Oncológicas, Academia Nacional de Medicina and [3]Instituto Angel Roffo, Buenos Aires, Argentina

[4]Present address: Molecular Carcinogenesis Unit, Oral and Pharyngeal Cancer Branch, National Institute of Dental and Craniofacial Research, Building 30, Room 213, National Institutes of Health, Bethesda, MD 20892-4340, USA

*To whom correspondence should be addressed at: Instituto de Biología y Medicina Experimental, Vuelta de Obligado 2490, C1428ADN Buenos Aires, Argentina. Tel: +54 11 4783 2869; Fax: +54 11 4786 2564; Email: clanari@dna.uba.ar

In this paper we demonstrate, using the C7-2-HI metastatic transplantable ductal mammary tumor, that endocrine therapy can induce complete regression of spontaneous lymph node and lung metastases in a mouse model of breast cancer progression. This tumor expresses high levels of estrogen and progesterone receptors and shows a high incidence of early axillary lymph nodes and lung metastases; using this model we had previously shown complete tumor regression of subcutaneous implants. Interestingly, although the metastases showed a more differentiated histology as compared with the primary growth, they underwent complete regression when treated with estrogens or antiprogestins. This phenomenon was associated with sustained cytostasis and apoptosis accompanied by increases in p21 and p27 expression and early tissue remodeling. These results highlight the essential role of PR in regulating cell proliferation in this model as well as its possible use as therapeutic target.

Introduction

Adjuvant therapy is defined as the treatment given in addition to the primary therapy to destroy any cancer cells that may have spread, even if they cannot be detected by radiology or laboratory tests; several studies have shown that adjuvant therapy for breast cancer may increase the chance of long-term survival by preventing a recurrence, http://cis.nci.nih.gov/fact/7_20.htm (1). Endocrine treatment such as tamoxifen (TAM) (2,3), and more recently first-generation aromatase inhibitors (4), are the adjuvant therapy of choice in operable breast cancer as well as in metastatic estrogen receptor alpha (ER) positive carcinomas (5). Interestingly, although the antiestrogen TAM has been used for decades with excellent results, post-menopausal women with breast cancer have also been successfully treated with estrogens, such as diethylstilbestrol or ethinyl estradiol (6–8). The exact mechanism by which TAM inhibits tumor growth is still not completely understood (9–12), although it is currently accepted that, as a selective estrogen receptor modulator or SERM, it behaves as an antiestrogen within the physiological context of the mammary gland. The pathways through which estrogens can inhibit the growth of a hormone-dependent breast cancer are also poorly understood. Experimental support for a growth-inhibitory action has been given by the facts that estrogen treatment induced complete regression in the T61 human xenograft model (13) and also in a T47D variant with overexpression of protein kinaseC alpha or PKC alpha (14). Even more controversial is the fact that antiprogestins may induce tumor regression in the same models in which antiestrogens inhibit tumor growth (15,16). The role of progesterone in breast cancer development has not been as thoroughly researched as the one of estrogen, although many experimental and epidemiological data available point toward a relevant one. The possible relevance of progestins has been highlighted by the results of the Women's Health Initiative (17) and the Million Women Study (18) that specifically link the use of progestins with human breast cancer.

In a previous publication we sought to evaluate the beneficial effects of estrogen and antiprogestins in mammary cancer, using a hormone-responsive model of breast cancer progression; we demonstrated that in BALB/c mice, mammary ductal carcinomas regress completely when treated with 17-β-estradiol (E_2) or antiprogestins (19–21) and partially when treated with TAM (22). This phenomenon is mediated by an important cytostatic effect accompanied by an increase in apoptosis (21). As the carcinomas in this model will eventually develop lymph node and lung metastases, we decided to extend our previous investigations to study the effects of endocrine treatment in advanced disease stages. This is a non-genetically manipulated model, especially suited to evaluate tumor progression (23–25) as the tumors evolve from a hormone-sensitive to a hormone-resistant state, a transition mimicking the acquisition of hormone resistance in human breast cancer. This transition is accompanied by distinctive changes in progesterone receptor (PR) expression; tumors which have acquired hormone independence but are still responsive to endocrine treatment express high levels of steroid receptors while unresponsive tumors show a different pattern of PR expression (26). Most of the experiments regarding hormone or antihormone action have been carried out using 3 or 4 human breast cancer cell lines out of more than 30 available, and in their respective xenografts in immunosuppressed mice (27–29) or in the rat methylnitrosourea (MNU) (30) or in the dimethylbenz[*a*]anthracene (DMBA) models (31). As progression models, these tumors have the

Abbreviations: DMBA, dimethylbenza[*a*]anthracene; ER, estrogen receptor alpha; hpf, high power fields; MNU, methylnitrosourea; MPA, medroxyprogesterone acetate; PR, progesterone receptor; s.c., subcutaneous; SERM, selective estrogen receptor modulator; TAM, tamoxifen; TUNEL, deoxynucleotidyl transferase-mediated dUTP–biotin nick end labeling.

†These two authors contributed equally to this work.

disadvantage of not giving rise to metastases, a fact that has been partially addressed, with the models generated in transgenic mice, but unfortunately most of them do not express ER and PR.

In this model we demonstrate that endocrine therapy can induce regression of tumor metastases, a process associated with cytostasis, apoptosis and expression of Cdk inhibitors.

Materials and methods

Experimental model

Animals. Two-month-old virgin female BALB/c mice (Instituto de Biología y Medicina Experimental Animal Facility) were used. The animals were housed in groups of four per cage in an air-conditioned room at $20 \pm 2°C$ under a 12 h light/dark cycle and access to food and tap water *ad libitum*. Animal care and manipulation were in agreement with institutional guidelines and the Guide for the Care and Use of Laboratory Animals (32).

Tumor. C7-2-HI is a metastatic transplantable ductal mammary tumor induced by the continuous administration of medroxyprogesterone acetate (MPA) to a BALB/c female mouse (23), maintained by serial subcutaneous (s.c.) transplantations into syngeneic female mice. It is a progestin-independent tumor that expresses high levels of ER and PR and shows a high incidence of early (40–60 days) spontaneous metastasis in homolateral axillary nodes and lung (33). The primary implants regressed completely after E_2 or antiprogestin treatment (21).

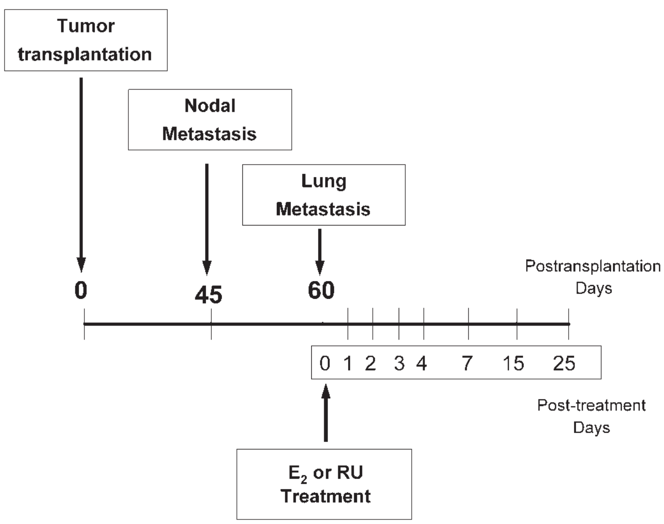

Fig. 1. Experimental design. C7-2-HI tumor transplanted subcutaneously in BALB/c mice originates lymph node metastasis after 45 days. All animals had lung metastases after 60 days. E_2 or RU pellets were s.c. implantations on day 60. Three animals per group were euthanized according to the schedule.

Treatments. Silastic pellets containing 5 mg of 17-β-estradiol (Sigma, St Louis, MI) or 6.5 mg of the antiprogestin RU 38486 (RU) (mifepristone: Sigma) were subcutaneously implanted as described previously (19–21).

Experimental design

Tumor samples were transplanted subcutaneously by a trocar into the right inguinal flanks of mice and the growth evaluated three times a week (length and width) with a Vernier caliper. Axillary node metastases were detectable by palpation ~45 days post-transplantation; at this time the size of the primary tumors was ~150 mm^2. Several animals were euthanized 60 days after tumor transplantation and the lungs evaluated histologically for metastases. After positive confirmation the treatments were started in the rest of the animals (Figure 1).

The mice were separated at random and sham operated or treated with E_2 ($n = 24$) or with RU ($n = 22$). From each group 3 or 4 animals were killed every day between days 1 and 4 and subsequently, on days 7, 15 and 25 post-treatment as shown in Figure 1. Control animals were euthanized on day 60, when treatments were initiated (Control 0, $n = 4$) and at the end of the experiment, on day 25 after treatment and on day 85 after tumor inoculum (Control 25 days, $n = 3$–4). Lymph nodes and lungs were fixed in 10% buffered formalin, embedded in paraffin and stained with Hematoxylin–Eosin (H&E) for histological diagnosis. Additional sections of 5 μm thickness were prepared for immunohistochemical studies. The number and size of pulmonary metastases were evaluated on histological sections.

Morphological studies. The morphology of tumor parenchyma (growth pattern, differentiation) and stroma, as well as mitosis and apoptosis were evaluated on H&E stained sections. The latter were counted in 10 and 15 high power fields (hpf), of each section using a 1000× magnification, and expressed as a mean ± standard deviation of the percentage of the ratios between the total number of events (mitosis or apoptosis) and the total cell number per hpf. Mitotic figures were identified morphologically by the condensed 'hairy' aspect of the chromosomes. Morphological identification of apoptosis was performed according to criteria previously reported (21); selected samples were also reacted using the deoxynucleotidyl transferase-mediated dUTP–biotin nick end labeling (TUNEL) method according to the manufacturer's instructions (Boehringer Mannheim, UK) (21). The number of lung metastases was evaluated in two non-consecutive histological sections using 10× objective. Only metastases with sizes >0.5 mm in diameter were included to evaluate the size decrease of lung metastases after treatment.

Immunohistochemistry. Sections of formalin-fixed, paraffin-embedded tissue were reacted with the different antibodies using the avidin-biotin-peroxidase complex technique (Vectastain Elite ABC kit; Vector Laboratories, Burlingame, CA). In brief, endogenous peroxidase activity was inhibited using 3% H_2O_2 in distilled water. Blocking solution (2% normal goat serum) was used before the specific antibody. Polyclonal antibodies to p21 (Oncogene Research Products, Boston, MA), p27 (C-19, Santa Cruz Biotechnology, Santa Cruz, CA), ER (MC-20, Santa Cruz Biotechnology) and PR (C-20, Santa Cruz Biotechnology) were used at 1:50 dilution and incubated overnight at room

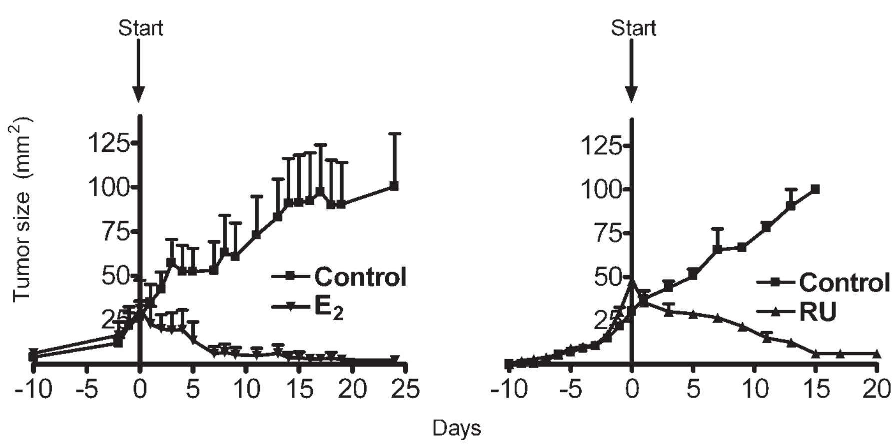

Fig. 2. Effects of E_2 or RU on lymph node metastatic growth. Mice bearing sc C7-2-HI tumor with lymph node homolateral metastasis of ~25–50 mm^2 were implanted with 5 mg E_2 pellets or 6.5 mg RU pellets. Growth curves showing axillary lymph nodes tumor sizes in E_2-treated (**left**) or RU-treated (**right**) mice ($n = 6$/group). Both treatments significantly reduced the size of metastases. Data are expressed as mean ± SD. The differences in tumor sizes were statistically significant since day 4, $P < 0.01$ E_2 versus control and day 6 RU versus control.

temperature. Microwave antigen retrieval (4 cycles of 5 min each in 0.1 M citrate buffer) using 750W Philips M902 microwave oven was used before p21 stain. The reaction was developed with 3, 3′-diaminobenzidine, 0.30 mg % in PBS with H_2O_2 to a final concentration of 0.5%, under microscopic control. Specimens were lightly counterstained with hematoxylin 10%, dehydrated and mounted. Quantification was performed as described above in Morphological studies.

Statistical analysis

Differences between groups in the number of mitosis, apoptosis or stained nuclei were evaluated using ANOVA followed by the Tukey *t*-test to compare differences between experimental and control groups. Mann–Whitney non-parametric test was used to compare the number of metastases.

Results

BALB/c mice bearing s.c. C7-2-HI tumors with axillary node metastasis were treated with E_2 or RU. Growth differences were evident enough to be detected as early as treatment day 2. The decrease in tumor size was more remarkable in E_2-treated mice than in RU-treated mice, since in the latter it took more time to induce complete tumor regressions (Figure 2).

To evaluate the effects of both agents on lung metastasis, randomly selected animals were euthanized at different times, according to the experimental design shown in Figure 1. Four out of six animals euthanized on day 25, showed complete metastases regression; only in one animal a metastasis with a size >0.5 mm was observed. The progressive decrease as well as the total number and the sizes observed in both groups are shown in Figure 3. The differences in both parameters were statistically significant ($P < 0.05$, Mann–Whitney test).

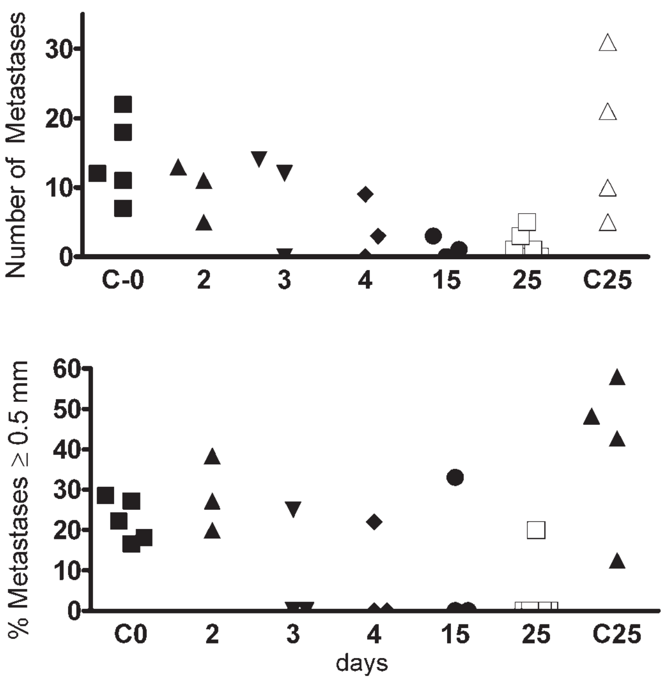

Fig. 3. Effect of E_2 treatment on lung metastasis. Mice bearing s.c. C7-2-HI tumor with lymph node homolateral metastasis of ~25–50 mm^2 and already established lung metastasis were implanted with 5 mg E_2 pellets or silastic pellets. Quantification of total number of metastases (**top**) and number of metastases >0.5 mm (**bottom**) during E_2-treatment until day 25 after pellet implantation. Control mice were euthanized at the moment of treatment initiation and at the end of the experiment, day 25. Different symbols were used to represent individual data at different times. Mann–Whitney test: $P < 0.05$ between 15 and 25 days in E_2-treated mice versus control (number of metastases) and $P < 0.05$ between E_2-treated and control (size) on day 25.

A similar trend was observed with RU and, as described for axillary node metastasis, this treatment was less efficient than E_2, since after 25 days of RU treatment regression was not complete in three out of four animals (data not shown).

Morphological features

C7-2-HI tumors growing subcutaneously were classified as ductal semi-differentiated carcinomas; node metastases showed a different pattern of growth, as they displayed the features of well-differentiated ductal carcinomas regardless of the size (Figure 4A and K). Lung metastases on the other hand, showed a poorly differentiated pattern forming nests of highly cohesive cells when they were small (when the treatment was

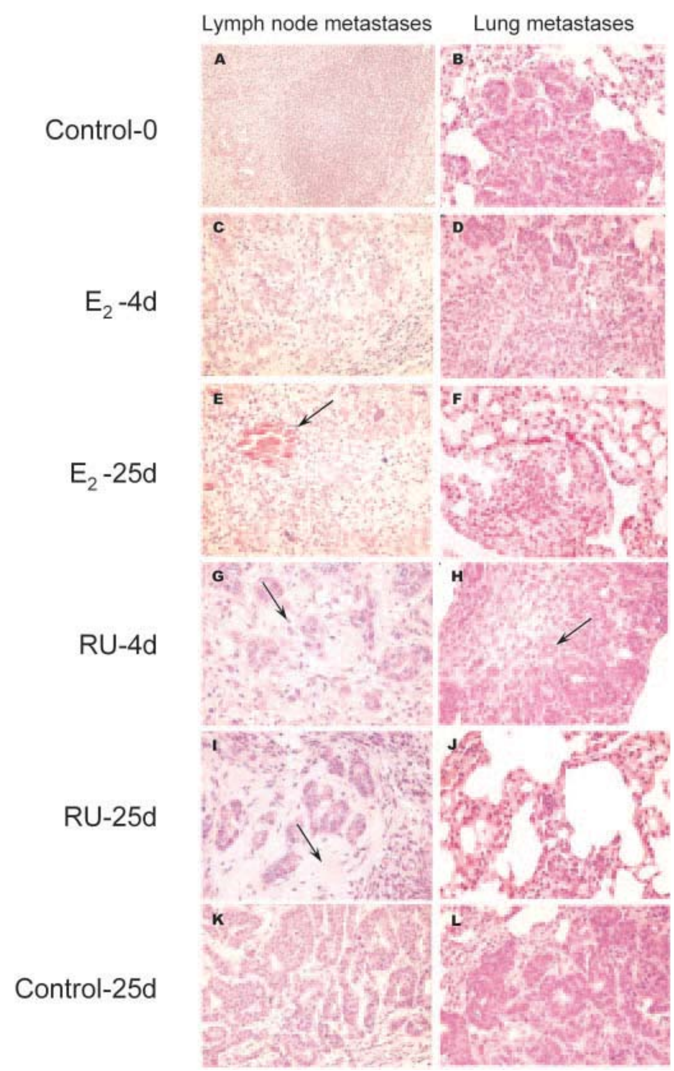

Fig. 4. Morphological features of C7-2-HI metastasis regression. Lymph node metastases (left panel) in control animals showed well differentiated ductal mammary carcinomas (**A**). On day 25 a higher glandular density was observed (**K**). Lymph node metastases treated for 4 days with E_2 (**C**) or RU (**G**) displayed abundant fibroblastic stroma and reduced number of glands. In late regressing metastasis, a small number of glands and calcification (**E**, arrow) or sclerohyalinosis (**I**, arrow) were observed. The histology of pulmonary metastases (right panel) was that of a ductal carcinoma in control animals (**B**), with a higher degree of differentiation at larger sizes (**L**). E_2 (**D**) or RU (**H**) treatment induced gland formation (arrow) already evident on treatment day 4. At the end of treatment only a few neoplastic cells surrounded by fibrosis and lymphocytes were observed (**F** and **J**). At early stages, foamy macrophages were conspicuous in all regressing metastases (G, arrow).

initiated) (Figure 4B) and a well-differentiated pattern at larger sizes (25 days later) (Figure 4L).

A progressive decrease in the number of tumor cells associated with an increase in stroma was observed in E_2- or RU-treated lymph node metastases (Figure 4C, E, G and I). After 4 days of treatment, the stroma consisted mainly of abundant extracellular matrix and fibroblasts; foci of calcification (Figure 4E, arrow) and sclerohyalinosis (Figure 4I, arrow) were also evident after 25 days of treatment. Inflammatory cells, such as granulocytes or lymphocytes, were not a conspicuous part of the stroma reaction. An extensive central necrosis was observed in node metastases of control mice, a phenomenon probably related to the size of the tumors, while only foci of necrosis were present in regressing node metastases.

As already mentioned, both treatments induced regression of pulmonary metastases, but E_2 treatment was much more effective than RU treatment. Few and isolated neoplastic cells were observed in lungs after 4–7 days in E_2-treated mice (Figure 4D). Lung metastasis treated with RU began to display glandular formation on day 4 post-treatment (Figure 4H, arrow) and on day 25 a few, small glands separated by increased fibrous tissue and lymphocytes were observed (Figure 4J). Necrosis was not observed in either treated or untreated lung metastases.

Foamy macrophages were observed in all regressing metastases after day 3 post-treatment (Figure 4G, arrow). Similar findings were reported previously in regressing tumors growing in s.c. tissue (21).

In lungs, where there is an increase of tumor differentiation with time, RU treatment induces an early differentiation that together with other phenomena will induce tumor regression. Differentiation alone is not a marker of quiescence in these tumors since untreated metastases show this differentiated phenotype.

Mitosis and apoptosis

Tumor metastasis regression was associated with a conspicuous cytostatic effect and an increase in apoptosis. The growth kinetics of both phenomena was similar in both organs for the same treatment (Figure 5). In E_2-treated animals lung metastases were studied only during the first 96 h, because at later times, owing to tumor regression, the number of remaining neoplastic cells was too small for meaningful analysis. In the case of RU treatment it took more time to duplicate the apoptotic index of controls in both axillary and lung metastases; these results were in agreement with those observed in the growth curves when comparing E_2 with RU treatment. The same happened with the mitotic index in which a 50% decrease was already observed at 24 h in E_2-treated mice ($P < 0.05$)

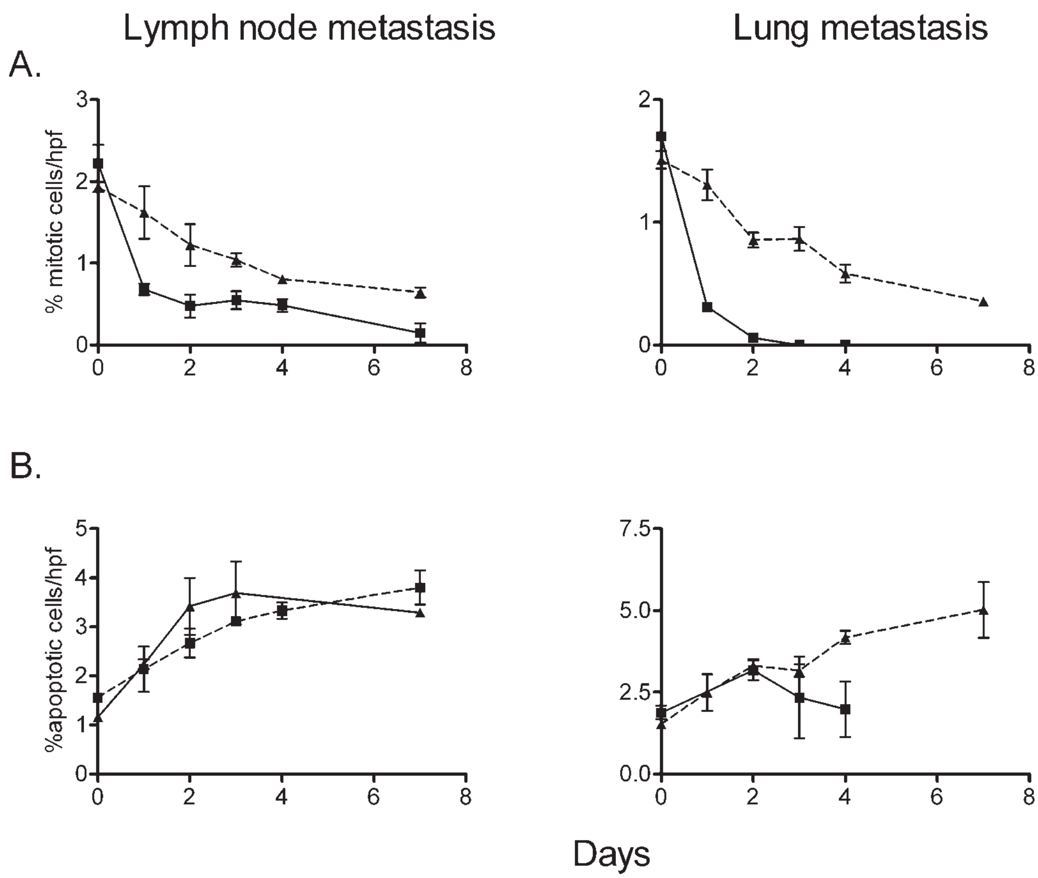

Fig. 5. Mitotic cells (**A**) and apoptotic cells (**B**) were counted in 10 or 15 hpf, respectively, of each section using a 1000× magnification, and expressed as a mean ± standard deviation of the percentage of the ratios between the total number of events (mitosis or apoptosis) and the total cell number per hpf. Mitotic figures were identified morphologically by the condensed 'hairy' aspect of the chromosomes and morphological identification of apoptosis was performed according to criteria previously reported (21). A significant decrease in mitosis was observed since the first day in E_2-treated metastasis ($P < 0.05$) and after 3 days in RU-treated metastasis ($P < 0.05$) and a significant increase in apoptosis was observed from day 2 in E_2- and RU-treated metastases ($P < 0.05$) ■, E_2; ▲, RU.

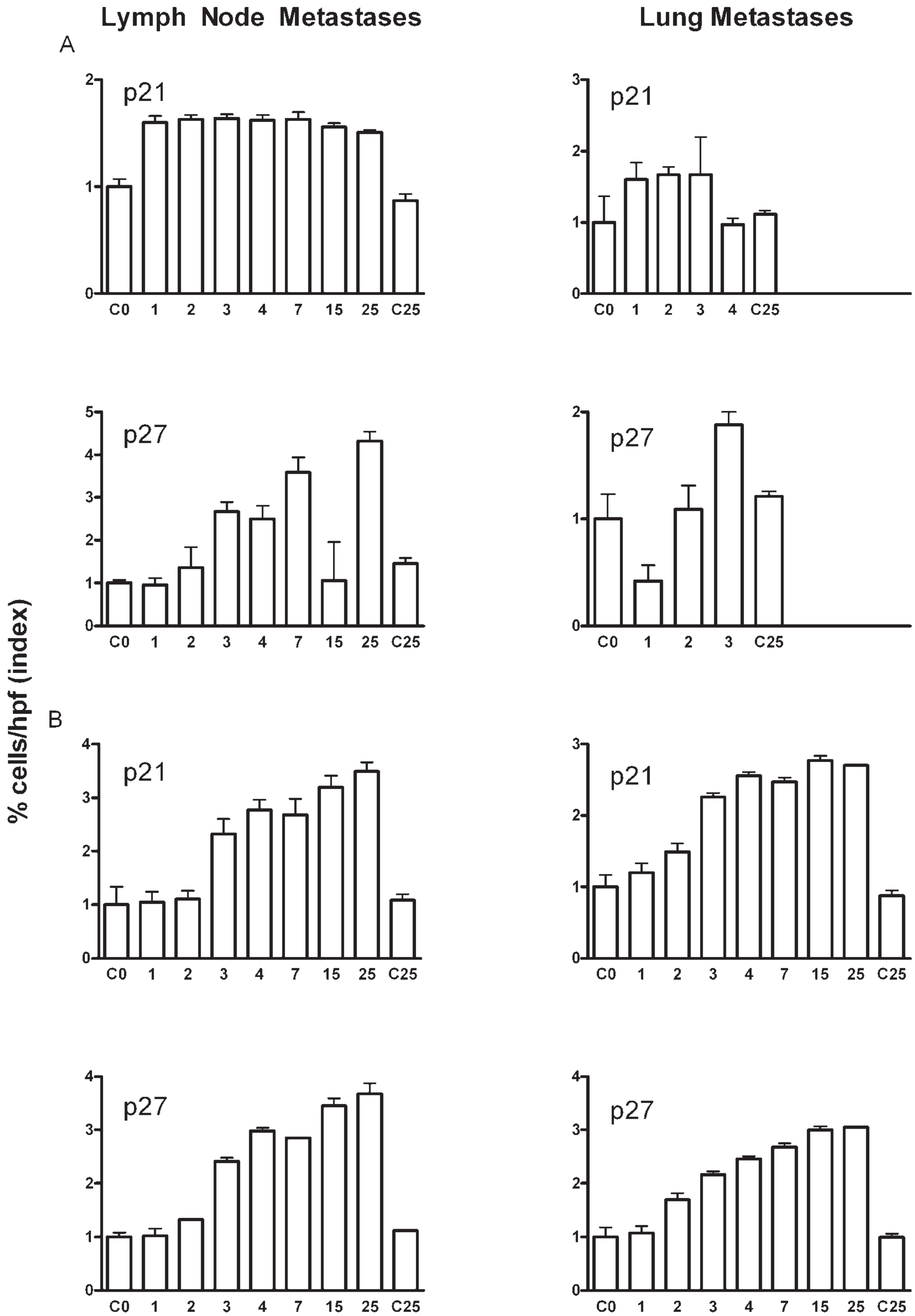

Fig. 6. p21 and p27 expressions (expressed as the ratio between the percentage of stained cells/hpf from experimental groups and the control group on day 0) in regressing lymph node and lung metastases of E_2-(**A**) and RU-treated mice (**B**). P21 significantly increased ($P < 0.01$) after 1 day of E_2 treatment in both lymph node and lung metastases while the increase in p27 was significant after 3 days ($P < 0.05$). In RU-treated mice the rise in p21 and p27 was significant after the third day of treatment ($P < 0.05$).

whereas it took >72 h to reach similar values in RU-treated mice ($P < 0.05$, Figure 5A–D).

p21 and p27 expression

In this study, we evaluated the kinetics of p21 and p27 expressions in axillary and lung metastases treated with E_2 or RU (Figure 6). The p21 levels were significantly increased and reached their peak after 24 h in axillary and lung metastases of E_2-treated mice ($P < 0.05$). In lymph node metastasis, p27 followed a similar trend, although the increase became statistically significant on day 3 and was not as even as p21. Moreover, an unexplained decrease was observed on day 15.

In lung metastasis, a statistically significant decrease in p27 expression was observed after the first day of treatment ($P < 0.05$) and the increase in p27 expression was observed on day 3 ($P < 0.001$). In RU-treated mice, p21 and p27 expressions in both axillary nodes and lungs followed a similar trend. As has been described previously for mitotic and apoptotic indices, the increase in p21 and p27 expressions was statistically significant ($P < 0.05$) after the third day of treatment. Representative immunostaining of p21 and p27 expressions in lymph node and lung metastases are shown in Figures 7 and 8, respectively. An early stage of an E_2-treated tumor and a late stage of an RU-treated tumor were selected. A high increase in

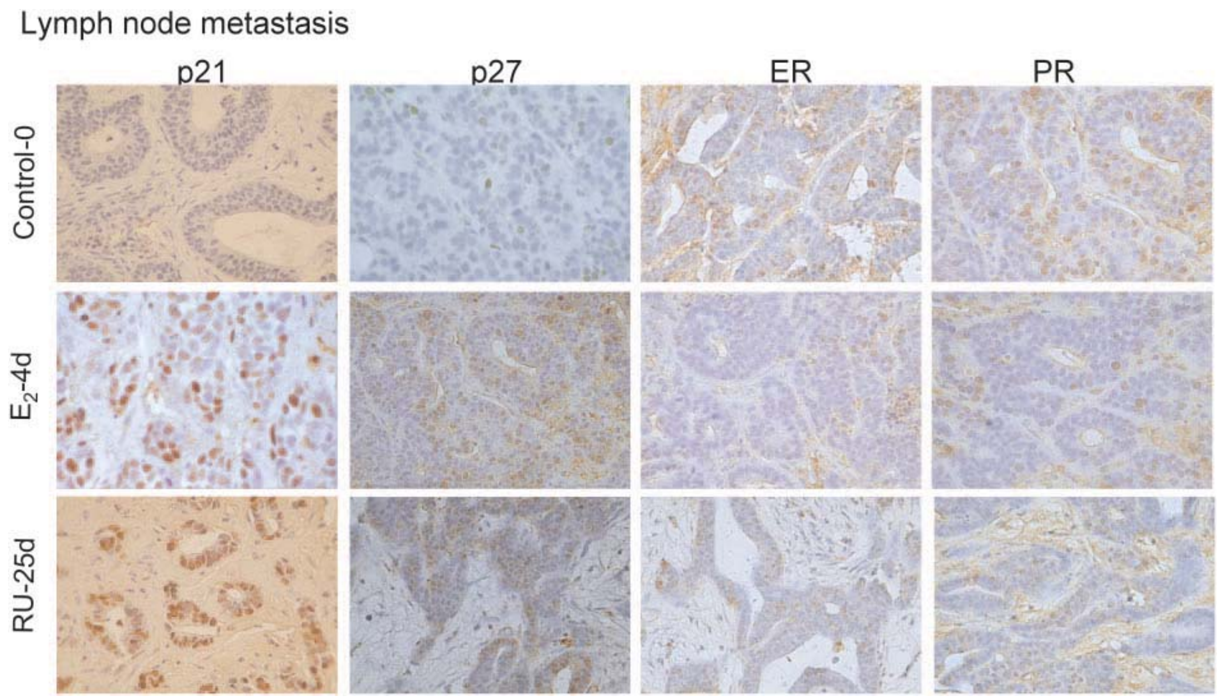

Fig. 7. Immunostaining of p21, p27, ER and PR in lymph node metastasis of C7–2-HI tumor treated or untreated with E_2 or RU. The experimental procedures as well as the antibodies used are described in Materials and methods.

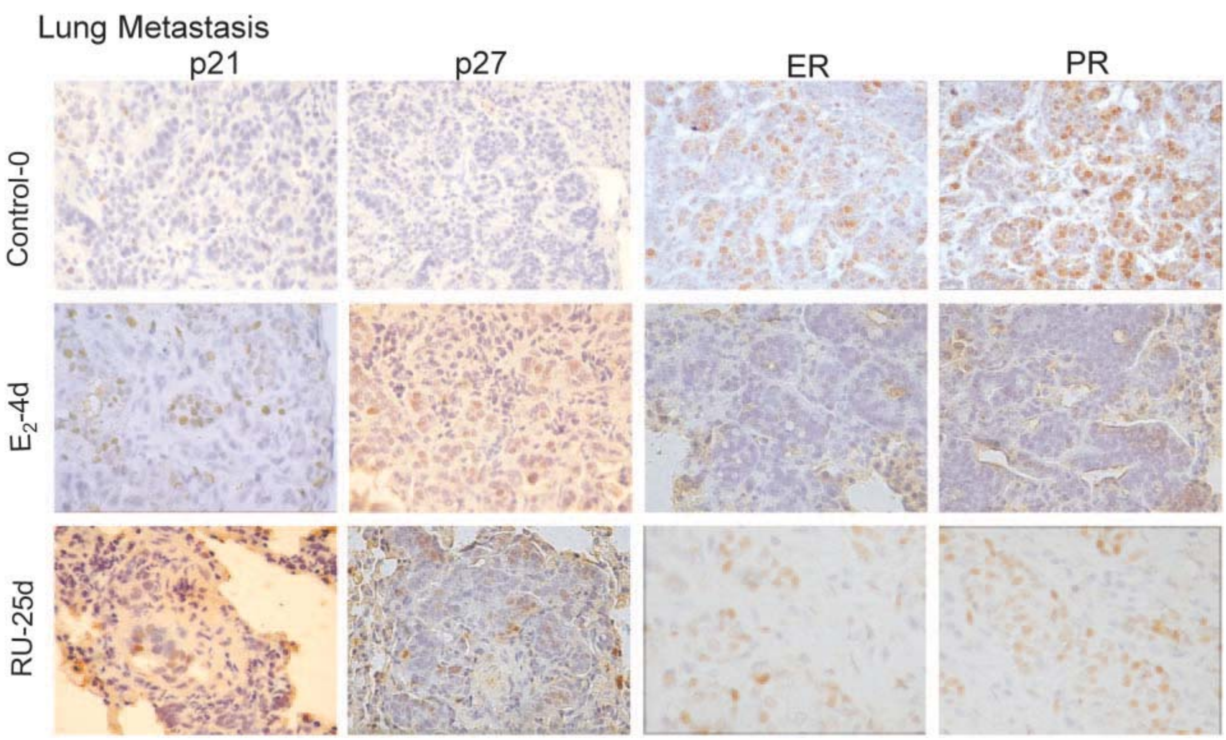

Fig. 8. Immunostaining of p21, p27, ER and PR in lung metastasis of C7–2-HI tumor treated or untreated with E_2 or RU. The experimental procedures and the antibodies used are described in Materials and methods.

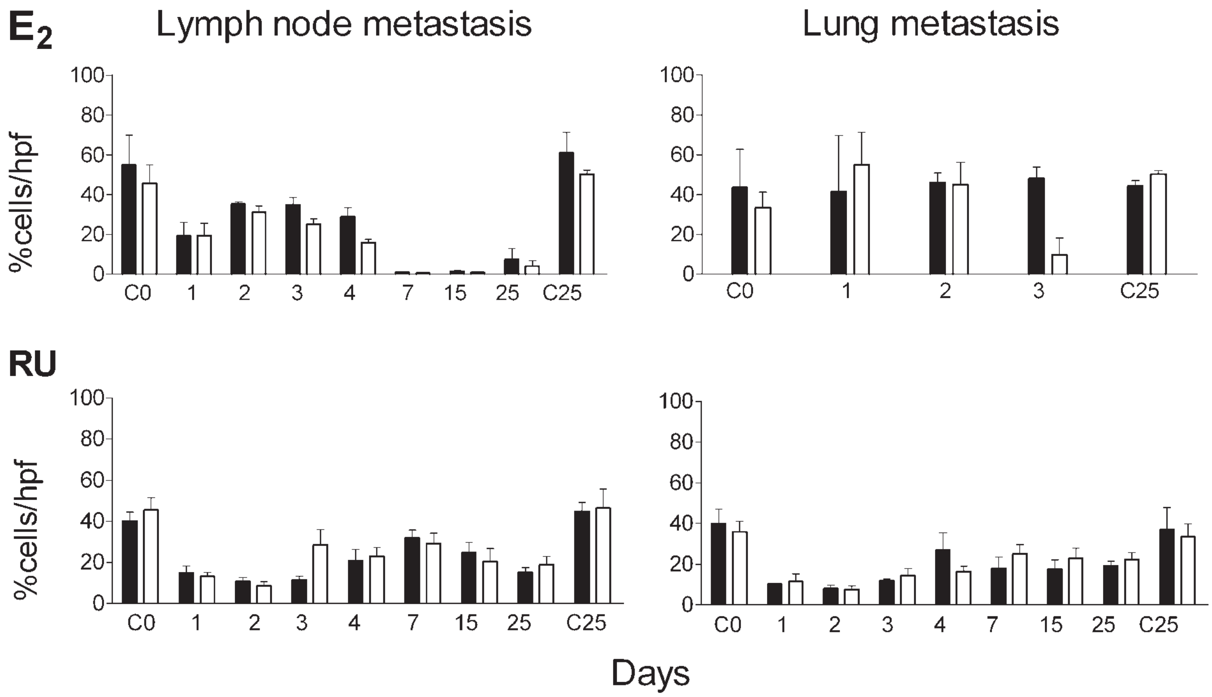

Fig. 9. ER (black bars) and PR (white bars) expressions, expressed as percentage of stained cells/hpf, in regressing lymph node and lung metastases of E_2- and RU-treated mice. Decrease in ER and PR expressions were statistically significant ($P < 0.05$) since day 1 after E_2 and RU treatment in lymph node metastasis and in RU-treated metastasis. In E_2-treated lung metastases the decrease in PR expression was significant on day 3 ($P < 0.05$).

nuclear staining can be observed in all E_2- or RU-treated tumors as compared with control tumors.

ER and PR expressions

The expression of ER and PR was significantly decreased in E_2- or RU-treated lymph node metastases as well as in RU-treated lung metastases. This inhibition was already observed 24 h after treatment (Figure 9). In lung metastases of E_2-treated mice this effect was not observed during the first 48 h although reduction in primary tumor sizes was already evident. The percentages of ER stained cells were very similar to those of PR regardless of the treatment or site of the metastases. Nuclear PR and ER staining in treated and untreated metastases are shown in Figures 7 and 8.

Discussion

In this paper we have explored the effects of hormone therapy in breast cancer metastases using a model of tumor progression in which experimental mammary ductal carcinomas, expressing ER and PR, metastasize to regional lymph nodes and lungs (33). As we have previously shown (21) the C7-2-HI tumor model is very suitable to evaluate hormone response, and in this context, we wanted to extend to the metastatic process our previous observations that primary tumors regressed with endocrine treatment. It is worthwhile pointing out that this is not a genetically engineered model, and not many are available to study all steps of tumor progression. Our results show that estrogen and antiprogestin treatment effectively induced regression of both axillary lymph node and lung metastases. This regression proceeded through cytostasis and increase in apoptosis with high levels of p21 and p27 expressions, as in primary tumors (21). In this model PR is an essential proliferative pathway; antiprogestin treatment (20) or treatment with PR antisense oligonucleotides (C.A. Lamb, L.A. Helguero, S. Giulianelli, R. Soldati, S.I. Vanzulli, A. Molinolo and C. Lanari, manuscript submitted) inhibit tumor growth. Even in tumors unresponsive to progestins, the proliferative effects of growth factors such as FGFs proceed through a cross-talk with the PR (34). Estrogens are also very effective in inhibiting tumor growth, although their mechanisms of action are still under investigation. We have found no histological differences between RU- and E_2-treated tumors, and the same is true for p21 and p27 expressions. Both RU and estrogens induced an inhibition in receptor expression in regressing tumors. Although the possibility arises that tumor regression may be associated with a decrease in steroid receptor expression, the data obtained in E_2-treated lung metastases, where an early decrease in tumor size was observed even in the absence of diminished levels of steroid receptor expression, suggests that the downregulation in receptors may be the consequence, rather than the cause of this phenomenon. An interesting finding was the fact that lymph node and lung metastases were histologically more differentiated, as compared with the primary implants. This higher degree of differentiation, however, did not correlate with any difference in hormone response. Experiments in which tumor cells were directly inoculated in lymphoid tissue and experiments in which tumor metastases were subcutaneously transplanted (data not shown), suggest that it is the organ in which the tumor is growing which confers the differentiated phenotype.

To our knowledge only a few reports are available exploring the regression of metastases in breast cancer. Among these, are the studies in the *neu* (35) and in the *wnt* 1 conditional transgenic mice (36) and those reported by Connolly *et al*. (37), in which the inhibition of cyclooxygenase reduced tumor growth and lung metastasis, although in this case only micrometastases were present at the time of treatment initiation.

Complete tumor regression was not achieved in these experiments, unlike what was reported in the *neu* conditional transgenic study (35), and the percentage of proliferating cells was similar in treated and untreated tumors. This lack of complete regression may be related to the failure of the model to induce sustained tumor cell apoptosis. In both the *neu* conditional transgenic model and in ours, the inhibition of the expression of a critical regulatory pathway i.e. *neu* and PR, is enough to induce complete regressions, demonstrating a hierarchical role for these pathways in the maintenance of the neoplastic phenotype. Interestingly, *neu* is also overexpressed in some of the tumors of our model (38) that also regress with estrogens and antiprogestins (C. Lanari, unpublished data).

Our data as well as that of others point toward the importance of hierarchical targets, the blockage of which would lead to sustained cytostasis and apoptosis. Triggering both phenomena will lead to tumor regression. Increases in p21 and p27 expressions are also behaving as markers of tumor regression at early stages. An increase in the expression level of these proteins after treatment initiation may result in a predictable assay to evaluate treatment responsiveness.

Acknowledgements

We are grateful to Miss Julieta Bolado for excellent technical assistance with animal handling. This work was supported by grants from SECYT (BID 1201/OC-AR, PICT 99 05-06389 and PICT 02 05-12276), Fundación Roemmers and Fundación Sales. C.L. and L.C. are members of Research Career CONICET, R.S. is fellow of SECYT and A.M. an associated researcher of Fundación Sales.

Conflict of Interest Statement: None declared.

References

1. National Cancer Institute (2004) Cancer Facts, Adjuvant Therapy for Breast Cancer: Questions and Answers.
2. Ward,H.W. (1973) Anti-oestrogen therapy for breast cancer: a trial of tamoxifen at two dose levels. *Br. Med. J.*, **1**, 13–14.
3. Ingle,J.N., Ahmann,D.L., Green,S.J. *et al*. (1981) Randomized clinical trial of diethylstilbestrol versus tamoxifen in postmenopausal women with advanced breast cancer. *N. Engl. J. Med*., **304**, 16–21.
4. Santen,R.J., Lipton,A. and Kendall,J. (1974) Successful medical adrenalectomy with amino-glutethimide. Role of altered drug metabolism. *JAMA*, **230**, 1661–1665.
5. Jordan,V.C. (1992) The strategic use of antiestrogens to control the development and growth of breast cancer. *Cancer*, **70**, 977–982.
6. Carter,A.C., Sedransk,N., Kelley,R.M., Ansfield,F.J., Ravdin,R.G., Talley,R.W. and Potter,N.R. (1977) Diethylstilbestrol: recommended dosages for different categories of breast cancer patients. Report of the Cooperative Breast Cancer Group. *JAMA*, **237**, 2079–2088.
7. Beex,L., Pieters,G., Smals,A., Koenders,A., Benraad,T. and Kloppenborg,P. (1981) Tamoxifen versus ethinyl estradiol in the treatment of postmenopausal women with advanced breast cancer. *Cancer Treat. Rep*., **65**, 179–185.
8. Brunner,N., Spang-Thomsen,M. and Cullen,K. (1996) The T61 human breast cancer xenograft: an experimental model of estrogen therapy of breast cancer. *Breast Cancer Res. Treat*., **39**, 87–92.
9. Jordan,V.C. (1994) Molecular mechanisms of antiestrogen action in breast cancer. *Breast Cancer Res. Treat*., **31**, 41–52.
10. Kessel,D. (1986) Interactions among membrane transport systems: anthracyclines, calcium antagonists and anti-estrogens. *Biochem. Pharmacol*., **35**, 2825–2826.
11. Sudo,K., Monsma,F.J.,Jr and Katzenellenbogen,B.S. (1983) Antiestrogen-binding sites distinct from the estrogen receptor: subcellular localization, ligand specificity, and distribution in tissues of the rat. *Endocrinology*, **112**, 425–434.
12. Arteaga,C.L., Koli,K.M., Dugger,T.C. and Clarke,R. (1999) Reversal of tamoxifen resistance of human breast carcinomas *in vivo* by neutralizing antibodies to transforming growth factor-beta. *J. Natl Cancer Inst*., **91**, 46–53.
13. Brunner,N., Spang-Thomsen,M., Vindelov,L. and Nielsen,A. (1983) Effect of 17 beta-oestradiol on growth curves and flow cytometric DNA distribution of two human breast carcinomas grown in nude mice. *Br. J. Cancer*, **47**, 641–647.
14. Chisamore,M.J., Ahmed,Y., Bentrem,D.J., Jordan,V.C. and Tonetti,D.A. (2001) Novel antitumor effect of estradiol in athymic mice injected with a T47D breast cancer cell line overexpressing protein kinase Calpha. *Clin. Cancer Res*., **7**, 3156–3165.
15. Schneider,M.R., Michna,H., Nishino,Y. and el Etreby,M.F. (1989) Antitumor activity of the progesterone antagonists ZK 98.299 and RU 38.486 in the hormone-dependent MXT mammary tumor model of the mouse and the DMBA- and the MNU-induced mammary tumor models of the rat. *Eur. J. Cancer Clin. Oncol*., **25**, 691–701.
16. Schneider,M.R., Michna,H., Nishino,Y. and el Etreby,M.F. (1990) Antitumor activity and mechanism of action of different antiprogestins in experimental breast cancer models. *J. Steroid Biochem. Mol. Biol*., **37**, 783–787.
17. Women's Health Initiative (2002) Risks and benefits of estrogen plus progestin in healthy postmenopausal women: principal results from the Women's Health Initiative randomized controlled trial. *JAMA*, **288**, 321–333.
18. Beral,V. and Million Women Study Collaborators (2003) Breast cancer and hormone-replacement therapy in the Million Women Study. *Lancet*, **362**, 419–427.
19. Kordon,E., Lanari,C., Molinolo,A.A., Elizalde,P.V., Charreau,E.H. and Pasqualini,C.D. (1991) Estrogen inhibition of MPA-induced mouse mammary tumor transplants. *Int. J. Cancer*, **49**, 900–905.
20. Montecchia,M.F., Lamb,C., Molinolo,A.A., Luthy,I.A., Pazos,P., Charreau,E., Vanzulli,S. and Lanari,C. (1999) Progesterone receptor involvement in independent tumor growth in MPA-induced murine mammary adenocarcinomas. *J. Steroid Biochem. Mol. Biol*., **68**, 11–21.
21. Vanzulli,S., Efeyan,A., Benavides,F., Helguero,L., Peters,G., Shen,J., Conti,C.J., Lanari,C. and Molinolo,A. (2002) p21, p27 and p53 in estrogen and antiprogestin-induced tumor regression of experimental mouse mammary ductal carcinomas. *Carcinogenesis*, **23**, 749–757.
22. Lamb,C.A., Helguero,L.A., Fabris,V., Lucas,C., Molinolo,A.A. and Lanari,C. (2003) Differential effects of raloxifene, tamoxifen and fulvestrant on a murine mammary carcinoma. *Breast Cancer Res. Treat*., **79**, 25–35.
23. Molinolo,A.A., Lanari,C., Charreau,E.H., Sanjuan,N. and Pasqualini,C.D. (1987) Mouse mammary tumors induced by medroxyprogesterone acetate: immunohistochemistry and hormonal receptors. *J. Natl. Cancer Inst*., **79**, 1341–1350.
24. Lanari,C., Kordon,E., Molinolo,A., Pasqualini,C.D. and Charreau,E.H. (1989) Mammary adenocarcinomas induced by medroxyprogesterone acetate: hormone dependence and EGF receptors of BALB/c *in vivo* sublines. *Int. J. Cancer*, **43**, 845–850.
25. Montecchia,M.F., Molinolo,A. and Lanari,C. (1999) Reversal of estrogen-resistance in murine mammary adenocarcinomas. *Breast Cancer Res. Treat*., **54**, 93–99.
26. Helguero,L.A., Viegas,M., Asaithamby,A., Shyamala,G., Lanari,C. and Molinolo,A.A. (2003) Progesterone receptor expression in medroxyprogesterone acetate-induced murine mammary carcinomas and response to endocrine treatment. *Breast Cancer Res. Treat*., **79**, 379–390.
27. Gottardis,M.M., Jiang,S.Y., Jeng,M.H. and Jordan,V.C. (1989) Inhibition of tamoxifen-stimulated growth of an MCF-7 tumor variant in athymic mice by novel steroidal antiestrogens. *Cancer Res*., **49**, 4090–4093.
28. Jordan,V.C. (1976) Antiestrogenic and antitumor properties of tamoxifen in laboratory animals. *Cancer Treat. Rep*., **60**, 1409–1419.
29. Wolf,D.M. and Jordan,V.C. (1994) Characterization of tamoxifen stimulated MCF-7 tumor variants grown in athymic mice. *Breast Cancer Res. Treat*., **31**, 117–127.
30. Gottardis,M.M. and Jordan,V.C. (1987) Antitumor actions of keoxifene and tamoxifen in the N-nitrosomethylurea-induced rat mammary carcinoma model. *Cancer Res*., **47**, 4020–4024.
31. Jordan,V.C. (1976) Effect of tamoxifen (ICI 46,474) on initiation and growth of DMBA-induced rat mammary carcinomata. *Eur. J. Cancer*, **12**, 419–424.
32. Institute of Laboratory Animal Resources,C.o.L.S.N.R.C. (1996) *Guide for the Care and Use of Laboratory Animals*. National Academy Press, Washington, DC.
33. Efeyan,A., Fabris,V., Merani,S., Lanari,C. and Molinolo,A.A. (2004) Establishment of two hormone-responsive mouse mammary carcinoma

cell lines derived from a metastatic mammary tumor. *Breast Cancer Res. Treat.*, **83**, 233–244.
34. Lamb,C., Simian,M., Molinolo,A., Pazos,P. and Lanari,C. (1999) Regulation of cell growth of a progestin-dependent murine mammary carcinoma *in vitro*: progesterone receptor involvement in serum or growth factor-induced cell proliferation. *J. Steroid Biochem. Mol. Biol.*, **70**, 133–142.
35. Moody,S.E., Sarkisian,C.J., Hahn,K.T., Gunther,E.J., Pickup,S., Dugan,K.D., Innocent,N., Cardiff,R.D., Schnall,M.D. and Chodosh,L.A. (2002) Conditional activation of Neu in the mammary epithelium of transgenic mice results in reversible pulmonary metastasis. *Cancer Cell*, **2**, 451–461.
36. Gunther,E.J., Moody,S.E., Belka,G.K., Hahn,K.T., Innocent,N., Dugan,K.D., Cardiff,R.D. and Chodosh,L.A. (2003) Impact of p53 loss on reversal and recurrence of conditional Wnt-induced tumorigenesis. *Genes Dev.*, **17**, 488–501.
37. Connolly,E.M., Harmey,J.H., O'Grady,T., Foley,D., Roche-Nagle,G., Kay,E. and Bouchier-Hayes,D.J. (2002) Cyclo-oxygenase inhibition reduces tumour growth and metastasis in an orthotopic model of breast cancer. *Br. J. Cancer*, **87**, 231–237.
38. Balana,M.E., Lupu,R., Labriola,L., Charreau,E.H. and Elizalde,P.V. (1999) Interactions between progestins and heregulin (HRG) signaling pathways: HRG acts as mediator of progestins proliferative effects in mouse mammary adenocarcinomas. *Oncogene*, **18**, 6370–6379.

Received January 6, 2005; revised February 17, 2005; accepted February 21, 2005